Thermal Creep of a Slightly Rarefied Gas through a Channel with Curved Boundary

C. J. T. Laneryd*, K. Aoki†, P. Degond** and L. Mieussens**

*Department of Aeronautics and Astronautics, Kyoto University, Kyoto 606-8501, Japan
†Department of Mechanical Engineering and Science
and Advanced Research Institute of Fluid Science and Engineering,
Kyoto University, Kyoto 606-8501, Japan
**MIP, Université Paul Sabatier, 31062 Toulouse cedex, France

Abstract. Thermal creep flows of a slightly rarefied gas induced in a channel with curved walls and with a large temperature variation are investigated numerically on the basis of the fluid-dynamic-type system that was derived systematically from the Boltzmann system by Sone *et. al.* [Phys. Fluids **8**, 628 (1996)], originally for the purpose of describing the ghost effect.

Keywords: Thermal Creep Flow, Rarefied Gas Flows, Slip Flows, Knudsen Compressor
PACS: 47.45.Gx, 47.45.-n, 47.45.Ab, 47.61.Cb, 51.10.+y

INTRODUCTION

Thermal creep is a flow of a slightly rarefied gas caused by the temperature gradient along a wall. Although it is one of the classical phenomena in rarefied gas dynamics [1], its importance was revived in recent years in connection with micro gas flows [2]. It is often analyzed by using the incompressible Navier–Stokes equations with the velocity slip in proportion to the temperature gradient along the wall. However, in order to derive correct fluid-dynamic-type systems, one has to carry out a systematic asymptotic analysis of the Boltzmann kinetic system for small Knudsen numbers based on a careful parameter setting [3]. For instance, when the temperature variation along the wall is large (more precisely, when the maximum temperature difference divided by a reference temperature is of the order of unity), some non Navier–Stokes terms should be included in the fluid-dynamic-type equations. The correct fluid-dynamic-type system (fluid-dynamic-type equations, their boundary conditions, and the correction inside the Knudsen layer) describing the thermal creep flow for large temperature variations has been derived in [3]. The aim of the present study is to apply this system to the thermal creep flows, caused by large temperature variations, in a channel with curved boundary. Our interest lies in the possibility of causing one-way flows in a channel with a periodic structure, which are relevant to the Knudsen compressor (cf. [4, 5, 6]).

It should be mentioned that the original purpose of deriving this system in [3] was to show the *ghost effect* in the continuum limit. That is, in spite of the fact that the flows caused by the effect of gas rarefaction (such as the thermal creep flow) vanish in this limit, their trace has a finite effect on the temperature field in the limit. A series of comprehensive studies of this effect has been performed by Sone and coworkers (see, e.g., [4, 5, 7]).

PROBLEM AND BASIC EQUATION

Let us consider a rarefied gas inside a channel with a curved wall and with a given temperature distribution (the shape of the channel and the temperature distribution will be specified later). We assume that: (i) no pressure gradient is imposed in the gas; (ii) the Knudsen number is small (i.e., the mean free path of the gas molecules is much smaller than any characteristic length in the system, e.g., the distance between the boundaries or the radius of curvature of the boundary); (iii) the temperature variation along the channel wall is finite (i.e., the maximum temperature difference divided by a reference temperature is of the order of unity); (iv) the gas molecules are hard spheres and undergo diffuse reflection on the channel wall. We investigate steady flows in the channel on the basis of the fluid-dynamic-type system that covers the present situation and was derived systematically from the Boltzmann system [3, 5].

Let T_{ref} and p_{ref} be, respectively, the temperature and pressure of the gas in the reference equilibrium state at rest, $\rho_{ref} = p_{ref}/RT_{ref}$ with R the specific gas constant, D_{ref} the reference length of the system, ℓ_{ref} the mean free path of the gas molecules at the reference state, and Kn the Knudsen number defined as $Kn = \ell_{ref}/D_{ref}$. Let $D_{ref}x_i$ denote the

rectangular space coordinates, $T_{\text{ref}}T$ the temperature, $p_{\text{ref}}p$ the pressure, $\rho_{\text{ref}}\rho$ the density, and $(2RT_{\text{ref}})^{1/2}u_i$ the flow velocity, so that x_i, T, p, ρ, and u_i are dimensionless quantities.

According to [5], the overall behaviour of the gas in the present situation can be described as follows. Any of the macroscopic quantities h of the gas (say, $h = T$, p, ρ, or u_i) can be expanded in a power series of a small parameter $\varepsilon = (\sqrt{\pi}/2)\text{Kn}$:

$$h = h_{(0)} + h_{(1)}\varepsilon + h_{(2)}\varepsilon^2 + \cdots. \tag{1}$$

In addition, it holds that

$$u_{i(0)} \equiv 0, \qquad p_{(0)} = \text{const}, \qquad p_{(1)} = \text{const}. \tag{2}$$

Then, the leading nontrivial terms of the expansions ($T_{(0)}$, $\rho_{(0)}$, $u_{i(1)}$, and $p_{(2)}$) are governed by the following fluid-dynamic-type equations:

$$\frac{\partial}{\partial x_i}\left(\rho_{(0)}u_{i(1)}\right) = 0, \tag{3}$$

$$\rho_{(0)}u_{j(1)}\frac{\partial u_{i(1)}}{\partial x_j} = -\frac{1}{2}\frac{\partial p^{\sharp}_{(2)}}{\partial x_i} + \frac{\gamma_1}{2}\frac{\partial}{\partial x_j}\left[T_{(0)}^{1/2}\left(\frac{\partial u_{i(1)}}{\partial x_j} + \frac{\partial u_{j(1)}}{\partial x_i} - \frac{2}{3}\frac{\partial u_{k(1)}}{\partial x_k}\delta_{ij}\right)\right]$$
$$+ \left[\frac{\Gamma_7}{\gamma_2}\frac{u_{j(1)}}{T_{(0)}^{3/2}}\frac{\partial T_{(0)}}{\partial x_j} - \frac{\Gamma_7}{4p_{(0)}T_{(0)}}\left(\frac{\partial T_{(0)}}{\partial x_j}\right)^2\right]\frac{\partial T_{(0)}}{\partial x_i}, \tag{4}$$

$$\rho_{(0)}u_{i(1)}\frac{\partial T_{(0)}}{\partial x_i} = \frac{\gamma_2}{2}\frac{\partial}{\partial x_i}\left(T_{(0)}^{1/2}\frac{\partial T_{(0)}}{\partial x_i}\right), \tag{5}$$

where

$$p^{\sharp}_{(2)} = p_{(2)} + \frac{2\gamma_3}{3p_{(0)}}\frac{\partial}{\partial x_k}\left(T_{(0)}\frac{\partial T_{(0)}}{\partial x_k}\right) - \frac{\Gamma_7}{6p_{(0)}}\left(\frac{\partial T_{(0)}}{\partial x_k}\right)^2, \tag{6}$$

$$\gamma_1 = 1.270042427, \quad \gamma_2 = 1.922284066, \quad \gamma_3 = 1.947906335, \quad \Gamma_7 = 1.758705. \tag{7}$$

[Γ_7 is defined as $\Gamma_7 = \gamma_3 - \gamma_7$ with the additional constant γ_7 that appeared in [3, 4]; the value of γ_7 in [3, 4] is incorrect, and the correct value ($\gamma_7 = 0.189201$) is given in [5].] The density $\rho_{(0)}$ and temperature $T_{(0)}$ are related through the equation of state,

$$\rho_{(0)} = p_{(0)}/T_{(0)}. \tag{8}$$

The boundary conditions for Eqs. (3)–(5) are given as

$$T_{(0)} = T_{\text{w}}, \qquad u_{i(1)} = -\frac{K_1 T_{\text{w}}^{1/2}}{p_{(0)}}\frac{\partial T_{\text{w}}}{\partial x_j}(\delta_{ij} - n_i n_j), \qquad \text{with} \quad K_1 = -0.6463, \tag{9}$$

where $T_{\text{ref}}T_{\text{w}}$ is the temperature of the channel wall, n_i its unit normal vector (pointing into the gas), and δ_{ij} the Kronecker delta. The constants $p_{(0)}$ and $p_{(1)}$ are to be chosen appropriately in each specific problem [note that $p_{(1)}$ does not affect Eqs. (3)–(5)].

The solution to the above fluid-dynamic-type system undergoes a correction in the Knudsen layer (a thin layer with thickness of a few mean free paths adjacent to the channel wall), the formula of which is omitted here.

NUMERICAL METHOD

The fluid-dynamic-type equations (3)–(5) bear a strong resemblance to the incompressible Navier–Stokes set of equations, since there is no obvious equation to solve to obtain the modified pressure $p^{\sharp}_{(2)}$ whose gradient appears in the momentum equation. The main differences are that the momentum equation contains an additional term corresponding to thermal stress, $\rho_{(0)}$ is not constant, and the boundary condition for $u_{i(1)}$ is of slip type. Previous numerical studies of the equations (3)-(5) has used a streamfunction-vorticity finite difference method [3, 8]. In the present study, however, we adopt a finite-volume approach because of its flexibility in application to complex geometries. Following [9] and some other appropriate references, we have adopted the finite-volume method for the incompressible Navier–Stokes system to the present fluid-dynamic-type system. In essence, it is a primitive variable approach for solving the equations, using a pressure-correction equation to ensure mass conservation. Because of the limited space, however, we omit further explanation of the scheme and give only the results of numerical analysis.

SOME NUMERICAL RESULTS AND DISCUSSION

In the present section, we show some results for the thermal creep flow obtained by solving the fluid-dynamic-type system, Eqs. (3)–(9), numerically. We consider only two-dimensional channels in the (x_1, x_2) plane. Instead of (x_1, x_2) and (u_1, u_2), we use (x, y) and (u_x, u_y), respectively. We also use the dimensional coordinate system $(x^*, y^*) = (D_{\text{ref}} x, D_{\text{ref}} y)$. We choose ρ_{ref} in such a way that the average of $\rho_{(0)}$ over the computational domain in the x-y space (see below) is unity.

One-way flow in a channel with sinusoidal walls

We first consider a gas in a two-dimensional channel with sinusoidal walls located at $y^* = \pm y_{\text{w}}^*$ with $y_{\text{w}}^* = [D_{\text{ref}} + d \cos(2\pi x^*/L)]$ $(0 < d < D_{\text{ref}})$ [Fig. 1(a)]. We assume that the wall temperature, which is common to both walls, has a sinusoidal distribution $T_{\text{w}} = T_{\text{ref}} - T_{\text{c}} \sin(2\pi x^*/L)$ $(0 < T_{\text{c}} < T_{\text{ref}})$. Taking into account the symmetry and periodicity of the flow field, we can reduce the computational domain to $0 \leq x^* \leq L$, $0 \leq y^* \leq y_{\text{w}}^*$ with the periodic condition at $x^* = 0$ and L, and the symmetry condition at $y^* = 0$.

This geometry corresponds to a variant of the Knudsen compressor (see [4, 5, 6]), so that a global unidirectional flow toward the right is expected to be induced. Figures 1(b), 1(c), and 1(d) show, respectively, the flow velocity $(u_{x(1)}, u_{y(1)})$, the isolines of $T_{(0)}$, and those of $p_{(2)}^{\sharp}$ in the case of $d/D_{\text{ref}} = 0.2$, $L/D_{\text{ref}} = 2$, and $T_{\text{c}}/T_{\text{ref}} = 0.5$. In Fig. 1(b), the arrow indicates the vector $(u_{x(1)}, u_{y(1)})$ at its starting point, and its scale is shown in the figure. We will comment on the dotted line in Fig. 1(c) in the last paragraph. Since $p_{(2)}^{\sharp}$ (or $p_{(2)}$) is determined only up to an additive constant at this stage, the constant in Fig. 1(d) has been chosen in such a way that the average of $p_{(2)}^{\sharp}$ over the domain is zero. Therefore, Fig. 1(d) provides only information about the gradient field of $p_{(2)}^{\sharp}$. The temperature gradient along the wall is leftward in the wider part and rightward in the narrower part. Therefore, the flow induced along the wall is leftward in the former part and rightward in the latter. However, the resultant flow is rightward in the bulk of the channel, and a counterclockwise circulating flow is formed near the wall in the wider part. Near the point of maximum temperature, there arises a very steep gradient of $p_{(2)}^{\sharp}$, which creates difficulties for the numerical solution method.

Let $m = 2 \int_0^{y_{\text{w}}^*/D_{\text{ref}}} \rho_{(0)} u_{x(1)} dy$, which is independent of x. Then, $m\varepsilon$ is the leading-order dimensionless mass-flow rate in the x direction [the Knudsen layer correction to $u_{x(1)}$, which is confined in a layer with thickness of $O(\varepsilon)$, contributes to the mass-flow rate only in the next order in ε]. The corresponding dimensional mass-flow rate (per unit thickness of the channel and per unit time] is given by $\rho_{\text{ref}}(2RT_{\text{ref}})^{1/2}D_{\text{ref}} m\varepsilon$. Figure 2(a) shows m versus d/D_{ref} for $T_{\text{c}}/T_{\text{ref}} = 0.5$ and 0.2 in the case of $L/D_{\text{ref}} = 2$, and Fig. 2(b) shows m versus L/D_{ref} for $d/D_{\text{ref}} = 0.3$ and $T_{\text{c}}/T_{\text{ref}} = 0.5$. It can be seen that there is an optimal choice of d to maximize the mass-flow rate. The dashed line in Fig. 2(a) shows the result for $T_{\text{c}}/T_{\text{ref}} = 0.5$ based on Eqs. (3)–(5) without the non-Navier–Stokes stress term (i.e., with $\gamma_3 = \Gamma_7 = 0$). The difference is small in the present problem but still visible.

If we consider the continuum limit $\varepsilon \to 0$, then the flow in the channel vanishes because of $u_{i(0)} \equiv 0$ [cf. Eq. (1)]. Therefore, the temperature field in the gas reduces to that of a stationary gas, which is known to be described by the steady heat-conduction equation. The isolines of the corresponding solution of the steady heat-conduction equation is shown by the dotted line in Fig. 1(c). On the other hand, the solution $T_{(0)}$ of the present fluid-dynamic-type system is nothing else than the temperature field in the continuum limit [cf. Eq. (1)]. However, it does not coincide with the solution of the heat-conduction equation. This discrepancy is caused by the infinitesimal velocity field, and it turns out that the heat-conduction equation, which does not contain this effect, cannot describe the temperature field in the stationary gas correctly. This is the ghost effect mentioned in the introduction, and the present problem is one example. The reader is referred to [4, 5, 7] for detailed information about this effect. Equations similar to Eqs. (3)–(5) had been derived in [10] in a more intuitive way for the purpose of demonstrating the convection caused by the thermal stress, but the ghost effect was not noticed there.

One-way flow in a channel of snaky shape

We next consider a two-dimensional channel of a periodic snaky shape with a uniform width, composed of alternating pieces of semi-circular segments and straight segments [Fig. 3(a)]. The temperature of the channel walls, which will be specified later, is also periodic with the same period as the channel shape. Let us consider the basic unit composed of a semi-circular and a straight segment defined as follows: The semi-circular segment is defined by

$$x^* = -(d^2 - y^{*2})^{1/2} \quad \text{(outer wall)}, \qquad x^* = -((d - D_{\text{ref}})^2 - y^{*2})^{1/2} \quad \text{(inner wall)}, \tag{10}$$
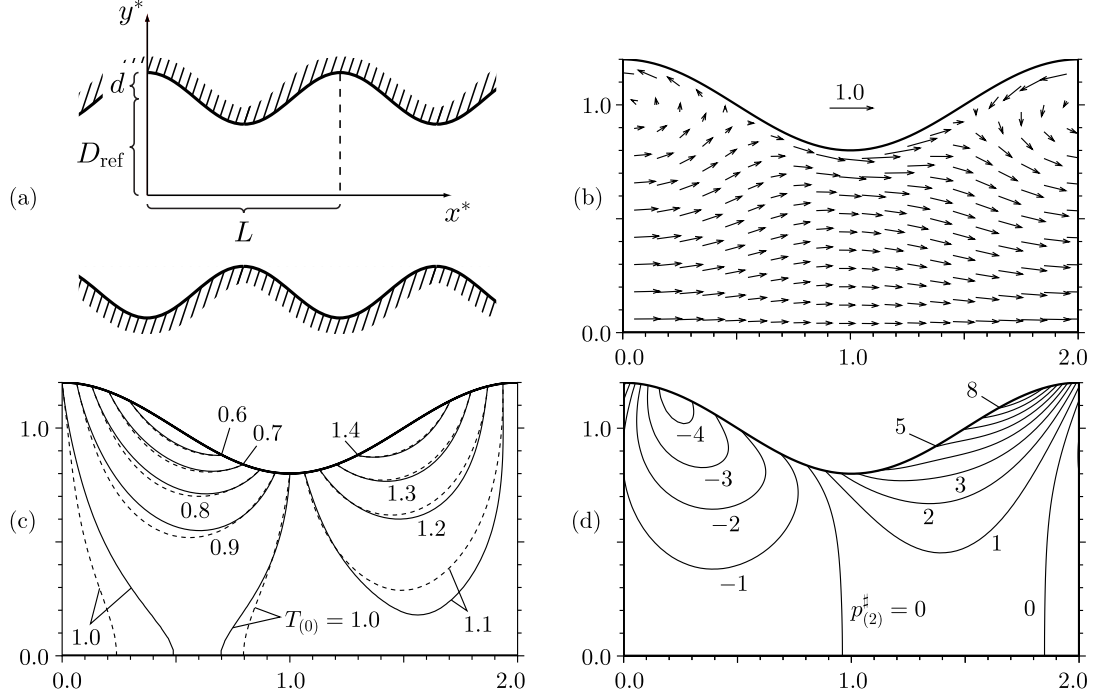
FIGURE 1. One-way flow through a channel with sinusoidal walls. (a) shows the channel geometry, whereas (b), (c) and (d) show the flow field for parameter values $d/D_{\mathrm{ref}} = 0.2$, $L/D_{\mathrm{ref}} = 2$, and $T_{\mathrm{c}}/T_{\mathrm{ref}} = 0.5$. (b) shows the flow velocity field with arrows indicating the vector $(u_{x(1)}, u_{y(1)})$ at its starting point. In (c) solid lines show isocurves of $T_{(0)}$, with dotted lines showing the solution of the heat-conduction equation for comparison. (d) shows isocurves of $p^{\sharp}_{(2)}$
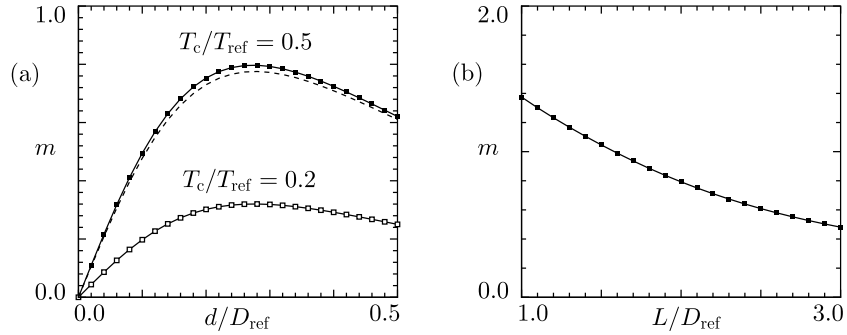
FIGURE 2. Parameter dependence of one-way mass flow m for a sinusoidal channel. (a) shows dependence on d/D_{ref} for $L/D_{\mathrm{ref}} = 2$. Black dots represent $T_{\mathrm{c}}/T_{\mathrm{ref}} = 0.5$, white dots $T_{\mathrm{c}}/T_{\mathrm{ref}} = 0.2$, and the dashed line the corresponding result for $T_{\mathrm{c}}/T_{\mathrm{ref}} = 0.5$ without the non-Navier–Stokes terms. (b) shows dependence on L/D_{ref} for $d/D_{\mathrm{ref}} = 0.3$ and $T_{\mathrm{c}}/T_{\mathrm{ref}} = 0.5$.

where D_{ref} is the channel width, and d ($d > D_{\mathrm{ref}}$) is the radius of the outer wall; the straight segment is defined by

$$y^* = d \quad \text{(outer wall)}, \qquad y^* = d - D_{\mathrm{ref}} \quad \text{(inner wall)}, \qquad (0 \leq x^* \leq L). \tag{11}$$

We assume that the wall temperature of the basic unit is highest at the connection of the two segments, i.e., at $(0, d)$ and $(0, d - D_{\mathrm{ref}})$, and lowest at both ends, i.e., at $(0, -d)$ and $(0, -d + D_{\mathrm{ref}})$ and at (L, d) and $(L, d - D_{\mathrm{ref}})$ and that it varies sinusoidally along the wall in each segment. That is, the wall temperature T_{w} is given by

$$T_{\mathrm{w}} = T_{\mathrm{ref}} + T_{\mathrm{c}} \frac{y^*}{(x^{*2} + y^{*2})^{1/2}} \quad \text{(semi-circular segment)}, \qquad T_{\mathrm{w}} = T_{\mathrm{ref}} + T_{\mathrm{c}} \cos \frac{\pi x^*}{L} \quad \text{(straight segment)}. \tag{12}$$
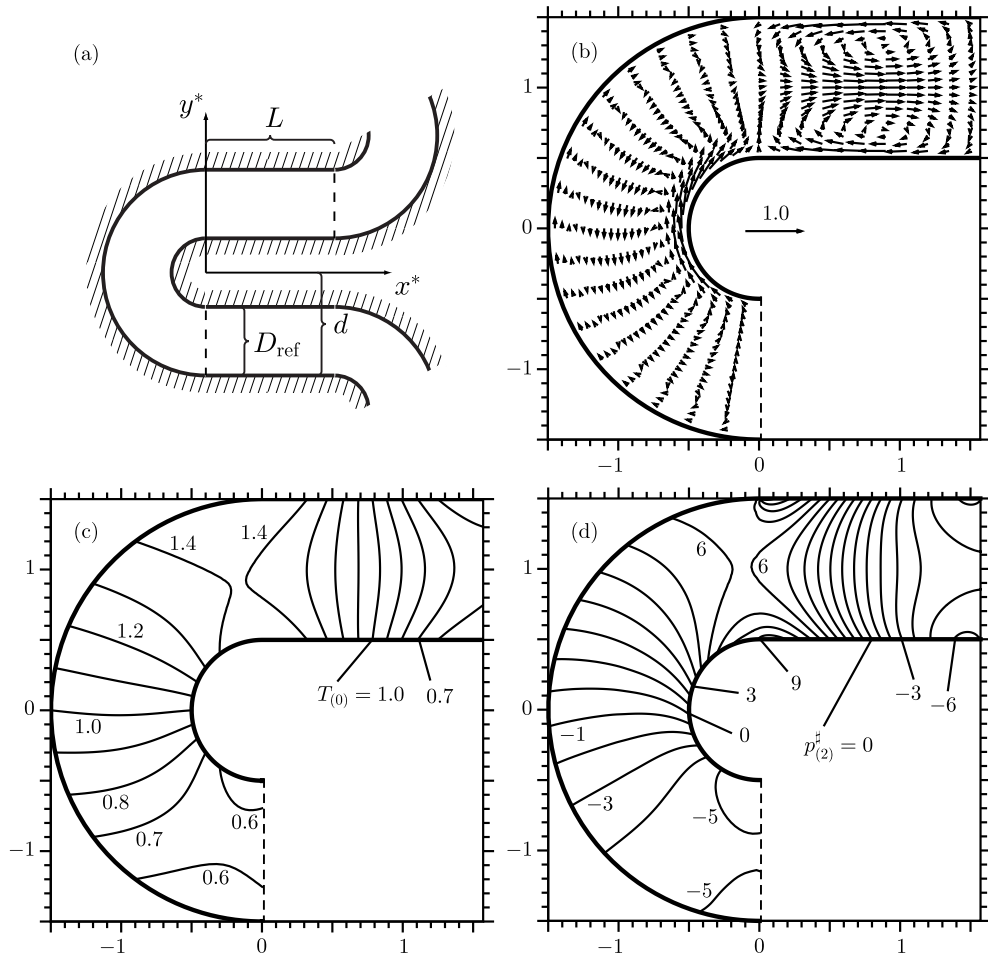
FIGURE 3. One-way flow through a channel of snaky shape. (a) shows the channel geometry, whereas (b), (c) and (d) show the flow field for parameter values $d/D_{\text{ref}} = 1.5$, $L/D_{\text{ref}} = \pi/2$, and $T_c/T_{\text{ref}} = 0.5$. (b) shows the flow velocity field with arrows indicating the vector $\left(u_{x(1)}, u_{y(1)}\right)$ at its starting point. (c) shows isocurves of $T_{(0)}$. (d) shows isocurves of $p_{(2)}^{\sharp}$
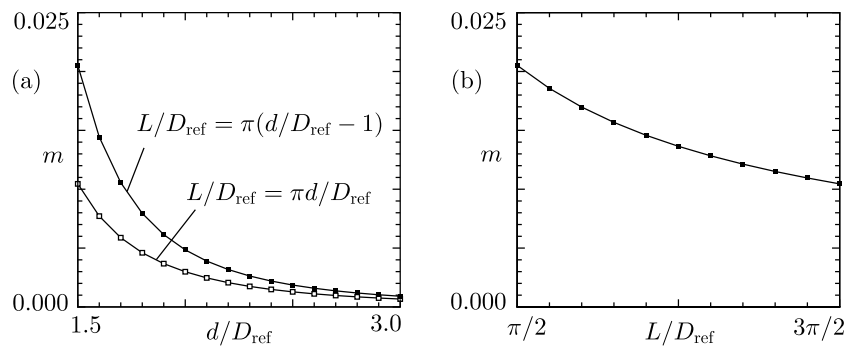
FIGURE 4. Parameter dependence of one-way mass flow m for a snake-shaped channel. (a) shows dependence on d/D_{ref} for $T_c/T_{\text{ref}} = 0.5$. Black dots represent $L/D_{\text{ref}} = \pi(d/D_{\text{ref}} - 1)$, and white dots $L/D_{\text{ref}} = \pi d/D_{\text{ref}}$. (b) shows dependence on L/D_{ref} for $d/D_{\text{ref}} = 1.5$ and $T_c/T_{\text{ref}} = 0.5$.

It is clear that the original periodic channel is geometrically composed of the above basic unit and its mirror image (with respect to y^* axis) with appropriate translation. We assume that the wall temperature of the original channel is also determined in the same way. Then, because of the periodicity and symmetry, we can solve the problem only in the basic unit by imposing appropriate conditions at both ends.

The present problem is motivated by recent attempts to make a Knudsen-type compressor using the change of curvature of the channel instead of the change of the channel width (cf. the problem in the previous subsection) [11, 12]. For a similar setting, a DSMC computation [11] as well as a deterministic computation [12] based on the BGK model has been performed, and a fluid-dynamic model has also been derived [12]. These computations show that a one-way net mass flow is caused for intermediate Knudsen numbers. However, since the mass-flow rate is smaller than the case of using the width change and, moreover, the induced flow becomes slower for smaller Knudsen numbers, it becomes increasingly difficult to confirm the one-way net mass flow with the decrease of the Knudsen number by means of the direct numerical computations. Therefore, the present study provides some pieces of information about the possibility of the one-way net mass flow for small Knudsen numbers.

In Figs. 3(b), 3(c), and 3(d), we show, respectively, the flow velocity $(u_{x(1)}, u_{y(1)})$, the isolines of $T_{(0)}$, and those of $p_{(2)}^{\sharp}$ in the case of $d/D_{\mathrm{ref}} = 1.5$, $L/D_{\mathrm{ref}} = \pi/2$, and $T_{\mathrm{c}}/T_{\mathrm{ref}} = 0.5$. In Fig. 3(b), the arrow indicates the vector $(u_{x(1)}, u_{y(1)})$ at its starting point, and its scale is shown in the figure. In Fig. 3(d), the additive constant of $p_{(2)}^{\sharp}$ is chosen in the same way as in Fig. 1(d). From Fig. 3(b), it is not clear whether there is a net one-way mass flow or not.

As in the previous problem, let $\rho_{\mathrm{ref}}(2RT_{\mathrm{ref}})^{1/2}D_{\mathrm{ref}}m\varepsilon$ be the dimensional mass-flow rate (per unit thickness of the channel and per unit time) in the clockwise direction in the basic unit (i.e., in the x^* direction in the straight segment). Figure 4(a) shows m versus d/D_{ref} for $L/D_{\mathrm{ref}} = \pi d/D_{\mathrm{ref}}$ (the case where the length of the straight segment is the same as that of the outer wall of the semi-circular segment) and $L/D_{\mathrm{ref}} = \pi(d/D_{\mathrm{ref}} - 1)$ (the case where the length of the straight segment is the same as that of the inner wall of the semi-circular segment) when $T_{\mathrm{c}}/T_{\mathrm{ref}} = 0.5$. Figure 4(b) shows m versus L/D_{ref} for $d/D_{\mathrm{ref}} = 1.5$ and $T_{\mathrm{c}}/T_{\mathrm{ref}} = 0.5$. These figures confirm that there is a net one-way mass flow, which is larger for a shorter straight segment. However, the mass-flow rate is much smaller than in the first problem.

We may incorporate the effect of the change of the width (cf. the first problem) to enhance the one-way mass flow. If we replace the inner wall of the semi-circular segment with a semi-ellipse to reduce the width at $y^* = 0$ by one half [keeping the temperature variation expressed by the first equation of Eq. (12)], the mass flow rate for $d/D_{\mathrm{ref}} = 1.5$ and $L/D_{\mathrm{ref}} = \pi(d/D_{\mathrm{ref}} - 1)$ in Fig. 4(a) or 4(b) becomes about 3 times ($2.05 \times 10^{-2} \to 6.62 \times 10^{-2}$). This increase is not so large as expected from the first problem. This may be due to the fact that the curved channel impedes the resulting one-way flow. However, the smaller mass-flow rate does not necessarily mean that the pumping effect is equally small when the channel is used as a Knudsen-type pump.

ACKNOWLEDGMENTS

REFERENCES

1. Sone, Y., J. Phys. Soc. Japan **21**, 1836 (1966); Ohwada, T., Sone, Y., and Aoki, K., Phys. Fluids A **1**, 1588 (1989).
2. Karniadakis, G., Beskok, A., and Aluru, N., *Microflows and Nanoflows: Fundamentals and Simulation* (Springer Science+Business Media, New York, 2005).
3. Sone, Y., Aoki, K., Takata, S., Sugimoto, H., and Bobylev, A. V., Phys. Fluids **8**, 628 (1996).
4. Sone, Y., Annu. Rev. Fluid Mech. **32**, 779 (2000).
5. Sone, Y., *Kinetic Theory and Fluid Dynamics*, Birkhäuser, Boston, 2002.
6. Sone, Y. and Sugimoto, H., in *Rarefied Gas Dynamics* (AIP, Melville, 2003), p. 1041.
7. Sone, Y., *Molecular Gas Dynamics: Theory, Techniques, and Applications* Birkhäuser, Boston, 2006.
8. Sone, Y., Handa, M. and Doi, T., Phys. Fluids **15**, 2903 (2003).
9. Ferziger, J. H. and Perić, M., *Computational Methods for Fluid Dynamics*, Springer-Verlag, Berlin, 2002.
10. Galkin, V. S., Kogan, M. N., and Friedlander, O. G., Izv. Akad. Nauk SSSR, Mekhanika Zhidkosti i Gaza **3**, 98 (1971).
11. Aoki, K., Degond, P., Mieussens, L., Nishioka, M., and Takata, S., this symposium.
12. Aoki, K., Degond, P., Mieussens, L., Takata, S., and Yoshida, H., in preparation.